ENVIRONMENTAL RESEARCH
CLIMATE

OPEN ACCESS

RECEIVED
14 April 2023

REVISED
6 August 2023

ACCEPTED FOR PUBLICATION
9 August 2023

PUBLISHED
25 August 2023

PAPER

Stronger Arctic amplification produced by decreasing, not increasing, CO_2 concentrations

Shih-Ni Zhou[1], **Yu-Chiao Liang**[1,2,*], **Ivan Mitevski**[3] **and Lorenzo M Polvani**[2,3,4]

[1] Department of Atmospheric Sciences, National Taiwan University, Taipei, Taiwan
[2] Lamont-Doherty Earth Observatory, Columbia University, Palisades, NY, United States of America
[3] Department of Applied Physics and Applied Mathematics, Columbia University, New York, NY, United States of America
[4] Department of Earth and Environmental Sciences, Columbia University, New York, NY, United States of America
[*] Author to whom any correspondence should be addressed.

E-mail: pamip.yuchiao@gmail.com and yuchiaoliang@ntu.edu.tw

Keywords: decreasing CO_2 concentrations, cold Arctic amplification, seasonality changes

Supplementary material for this article is available online

Abstract

Arctic amplification (AA), referring to the phenomenon of amplified warming in the Arctic compared to the warming in the rest of the globe, is generally attributed to the increasing concentrations of carbon dioxide (CO_2) in the atmosphere. However, little attention has been paid to the mechanisms and quantitative variations of AA under decreasing levels of CO_2, when cooling where the Arctic region is considerably larger than over the rest of the planet. Analyzing climate model experiments forced with a wide range of CO_2 concentrations (from 1/8× to 8×CO_2, with respect to preindustrial levels), we show that AA indeed occurs under decreasing CO_2 concentrations, and it is stronger than AA under increasing CO_2 concentrations. Feedback analysis reveals that the Planck, lapse-rate, and albedo feedbacks are the main contributors to producing AAs forced by CO_2 increase and decrease, but the stronger lapse-rate feedback associated with decreasing CO_2 level gives rise to stronger AA. We further find that the increasing CO_2 concentrations delay the peak month of AA from November to December or January, depending on the forcing strength. In contrast, decreasing CO_2 levels cannot shift the peak of AA earlier than October, as a consequence of the maximum sea-ice increase in September which is independent of forcing strength. Such seasonality changes are also presented in the lapse-rate feedback, but do not appear in other feedbacks nor in the atmospheric and oceanic heat transport processeses. Our results highlight the strongly asymmetric responses of AA, as evidenced by the different changes in its intensity and seasonality, to the increasing and decreasing CO_2 concentrations. These findings have significant implications for understanding how carbon removal could impact the Arctic climate, ecosystems, and socio-economic activities.

1. Introduction

During the past 40 years, observational records indicated that the near-surface air temperature in the Arctic has risen 2–4 times more than that in the rest of globe (Serreze and Francis 2006, Serreze *et al* 2009, Lenssen *et al* 2019, Meredith *et al* 2019, England *et al* 2021, Chylek *et al* 2022, Rantanen *et al* 2022). This phenomenon, the so-called Arctic amplification (AA), is widely attributed to the increasing concentration of carbon dioxide (CO_2) in the atmosphere (Manabe and Wetherald 1975, Gillett *et al* 2008, Jones *et al* 2013, Previdi *et al* 2020, Taylor *et al* 2022), although other greenhouse gases (notably halocarbons) may also have contributed (Polvani *et al* 2020, Liang *et al* 2022b). Future projections with the state-of-the-art climate models forced by standard warming scenarios also robustly indicate that AA will persist and increase in coming decades, with its annual-mean value peaking in the early 21st century (Collins *et al* 2013, Davy and Outten 2020, Cai *et al* 2021, Holland and Landrum 2021, Taylor *et al* 2022, Wu *et al* 2023). More

importantly, the amplified Arctic warming has exerted profound influences on local weather, ecosystems, and socio-economic activities within the Arctic Circle (Whiteman and Yumashev 2018, Burgass *et al* 2019, Meredith *et al* 2019, Alvarez *et al* 2020), and there has been vigorous debate on whether or not it can affect weather extremes and climate variability in the Northern Hemisphere mid-latitudes (Francis and Vavrus 2012, Barnes 2013, Cohen *et al* 2014, 2018, 2020, Mori *et al* 2014, Barnes and Screen 2015, Overland *et al* 2015, 2016, Coumou *et al* 2018, Blackport *et al* 2019, Blackport and Screen 2020a, 2020b, Zappa *et al* 2021, Smith *et al* 2022). Advancing our knowledge of AA and the contributing factors, therefore, is not only important for regional impacts, but also carries significant global implications.

While most studies focused on the AA forced by the increasing concentration of atmospheric CO_2 at century-long timescales (e.g. Pithan and Mauritsen 2014, Dai *et al* 2019, Previdi *et al* 2020, Hu *et al* 2022, Liang *et al* 2022a), less attention has been devoted to investigating the mechanisms linking decreasing amounts of CO_2 to AA. In such scenarios one might expect amplified Arctic cooling compared to the rest of the globe. Recent studies regarding the effects of aerosol emissions on global or Arctic climate revealed the possibility of AA appearance in the cooling scenario (Deng *et al* 2020, Jiang *et al* 2020, England *et al* 2021). In paleoclimate studies, on the other hand, the AA signature has been shown to emerge during the periods of both decreasing and increasing CO_2 levels. For example, Hoffert and Covey (1992) and Miller *et al* (2010) quantified the magnitude of AA during the holocene thermal maximum, last glacial maximum, last interglacial, and middle pliocene using paleoclimate proxies. Also in paleoclimate modelling studies, the appearance of AA has been simulated in both warming and cooling scenarios (Sloan and Rea 1996, Park *et al* 2019). However, a comprehensive analysis to examine its underlying drivers, and to directly contrast the phenomenological and mechanical differences in AA produced by cooling forcers has not yet been conducted to date.

Furthermore, AA exhibits a unique seasonal dependence, characterized by its disappearance in boreal summer, emergence in early autumn, and peak in late autumn and winter (Manabe and Stouffer 1980, Lu and Cai 2009b, Boeke and Taylor 2018, Chung *et al* 2021, Holland and Landrum 2021, Taylor *et al* 2022, Liang *et al* 2022a). Recent studies highlighted that the seasonality of AA can be altered—with its peak value gradually shifting from autumn into winter—as CO_2 or other greenhouse gas concentrations increase (Liang *et al* 2022a, Wu *et al* 2023); it has been shown that this is due to changes in sea-ice effective heat capacity (Hahn *et al* 2022). However, no attention has been paid to the change of AA seasonality in a cooling scenario. Does the peak month of AA shift backward from autumn to summer forced by CO_2 reduction? What is the mechanism responsible for AA seasonality change under decreasing CO_2 concentrations? These questions remain unanswered and deserve further studies.

The novelty of this study is to examine AA forced by decreasing CO_2 concentrations, building upon a previous study that has analyzed the influences of increasing CO_2 concentrations on AA and its seasonality (Liang *et al* 2022a). We contrast the phenomenological and mechanical characteristics of AA driven decreasing CO_2 concentrations with those from increasing CO_2. We also perform a detailed feedback analysis, to shed insight onto the underlying mechanisms that produce stronger AA under decreasing CO_2 concentrations. We then look into AA seasonality change under CO2 forcing with a focus on the migration of the peak value within one year. Finally, we discuss the results in the context of asymmetric Arctic responses to warming and cooling anthropogenic forcers. Throughout this manuscript, we refer to AA produced by decreasing CO_2 concentrations as cold AA, while that by increasing CO_2 levels as warm AA.

2. Methods

This study analyzes a series of fully-coupled atmosphere-ocean-sea-ice-land model experiments under a wide range of abrupt CO_2 forcings (Mitevski *et al* 2021, 2022). We use the Community Earth System Model version 1 (CESM1, Kay *et al* 2015), consisting of the Community Atmosphere Model version 5 (CAM5), the Community Ice CodE version 4 (CICE4), the Community Land Model version 4 (CLM4), and the parallel ocean program version 2 (POP2) with nominal 1° horizontal resolution in all components. The model is forced with decreasing and increasing CO_2 concentrations in the atmosphere: 0.125x, 0.25x, 0.5x, 1x (i.e. preindustrial (PI) CO_2 level), 2x, 3x, 4x, 5x, 6x, 7x, 8xCO_2 of PI concentration level. All other trace gases, ozone concentrations, and aerosols are fixed at their PI values. The simulations follow the 4xCO_2 protocol for the Coupled Model Intercomparison Project Phase 6 (CMIP6, Eyring *et al* 2016), so that 150 year integration is conducted for each experiment starting from PI initial conditions. In our analyses, the response is defined as the difference (hereafter Δ) of any variable between the nxCO_2 run and the 1xCO_2 run (i.e. the PI control run). We average the response over the last 30 years to present the mean response. We also average the response over the last 60 years and obtain similar results, corroborating that the response is not sensitive to different chosen periods.

To quantify the strength of AA, we compute a non-dimensional factor (hereafter AAF):

$$\mathrm{AAF} = \frac{\Delta \mathrm{SAT}_{\mathrm{Arctic}}}{\Delta \mathrm{SAT}_{\mathrm{global}}}, \tag{1}$$

where $\Delta \mathrm{SAT}_{\mathrm{Arctic}}$ denotes the surface-air temperature (SAT) response averaged over the Arctic domain (60°–90°N), while $\Delta \mathrm{SAT}_{\mathrm{global}}$ the global-averaged SAT response. This AAF definition has been widely used and its physical interpretation has been discussed in many AA studies using abrupt CO_2 experiments (e.g. Pithan and Mauritsen 2014, Goosse *et al* 2018, Liang *et al* 2022a).

To investigate the underlying mechanism contributing to AA, we perform the feedback analysis adopting the top-of-atmosphere (TOA) energy budget over the Arctic domain (60°–90°N) and tropical domain (30°S–30°N) (Soden *et al* 2008). We consider the energy budget equation for the atmospheric column:

$$\Delta R + \Delta F - \Delta H_o = 0, \tag{2}$$

where ΔR is the response of net downward radiation at the TOA, ΔF is that of horizontal convergence of atmospheric and oceanic energy transports combined, and ΔH_o is that of ocean heat uptake. We estimate the net ocean heat storage by ΔH_o solely because the atmosphere heat capacity, land heat uptake, and melting of snow and ice can be neglected due to small heat capacities (Polvani *et al* 2020, Liang *et al* 2022b). We consider ΔF as the residual of the energy budget and estimate it as the difference between ΔR and ΔH_o. Following previous studies (e.g. Pithan and Mauritsen 2014, Polvani *et al* 2020, Hahn *et al* 2021, Jenkins and Dai 2021, Beer and Eisenman 2022, Liang *et al* 2022b, Wu *et al* 2023), we further decompose ΔR into:

$$\Delta R = \Delta R_{\mathrm{F}} + \Delta R_{\mathrm{PL}} + \Delta R_{\mathrm{LR}} + \Delta R_{\mathrm{AL}} + \Delta R_{\mathrm{WV}} + \Delta R_{\mathrm{CL}}, \tag{3}$$

where ΔR_{PL}, ΔR_{LR}, ΔR_{AL}, ΔR_{WV}, and ΔR_{CL} represents the contributions of Planck, lapse-rate, albedo, water vapor, and cloud feedbacks to ΔR, respectively. In this study, we use the radiative kernels of CAM5 (Pendergrass *et al* 2018) to perform the ΔR decomposition. To estimate the effective radiative forcing (ERF) ΔR_{F}, we use the corresponding set of fixed-SST runs with varying CO_2 concentrations and take the last 30 year mean difference between the TOA energy fluxes (Mitevski *et al* 2021). Lastly, the response of oceanic heat transport (ΔOHT) is approximated as the difference between ΔH_o and the response of net surface heat fluxes (sum of shortwave and longwave radiation, and sensible and latent heat fluxes) between the ocean and atmosphere. The response of atmospheric heat transport (ΔAHT) is calculated as the difference between ΔF and ΔOHT. All terms are converted to temperature responses dividing by negative global mean Planck feedback parameter $-\overline{\lambda_{\mathrm{PL}}}$ following Pithan and Mauritsen (2014) and Goosse *et al* (2018). We estimate the residual of the kernel approximation as the difference between the TOA radiative flux change and the sum of these feedback contributions.

The statistical significance is informed with the error bars or color shadings shown in figures 2–5 using a Student's t-distribution with 95% confidence intervals. The sample size of the variables is 30, considering the annual-mean values in the last 30 years. If the two error bars of two variables do not overlap, their means are called statistically separable in this study. For the feedback analysis, we apply a bootstrapping technique (Pedregosa *et al* 2011) to randomly sample 30 year means 10 000 times with replacement to provide the uncertainty estimation shown in figures 3(a) and (b).

3. Results

We begin by looking into the time series of annual-mean Arctic and global SATs during the 150 year integration period (figure 1(a)). As expected in the abrupt CO_2 experiments, both Arctic and global SATs under different CO_2 levels adjust quickly in the first 30 years, and then gradually evolve towards quasi-equilibrium states. In the last 30 years, for example, the Arctic cooling effect in $0.125\times CO_2$ run gives Arctic SAT 244 K, 16 K lower than the SAT in $1\times CO_2$ run; whereas the $8\times CO_2$ warming effect leads to 278 K, 18 K higher than the SAT of $1\times CO_2$ run. Correspondingly, the sea-ice extent (SIE) grows and declines (figure 1(b)): in particular, the $7\times CO_2$ and $8\times CO_2$ forcings melt sea ice rapidly in the first 15 years and lead to an ice-free condition (less than 1 million km^2 SIE, grey shading in figure 1(b) afterward, while reducing CO_2 concentration gives a gentle SIE increase with time. The degree to which the sea ice responds reflects the CO_2 forcing strength. We further find that the cold AAFs are larger than the warm ones throughout most of 150 years (figure 1(c)). It is a rather surprising result because one may naively imagine that the climate system responds to warming and cooling forcers similarly, giving rise to similar AAF. Thus, understanding why weakening CO_2 forcing, rather than enhancing, leads to stronger AA is the main purpose of this study.

We next focus on the last 30 year mean responses of Arctic SAT, SIE, and turbulent heat fluxes (latent plus sensible heat fluxes) in order to illustrate their coupled relationships and reveal the mechanism under

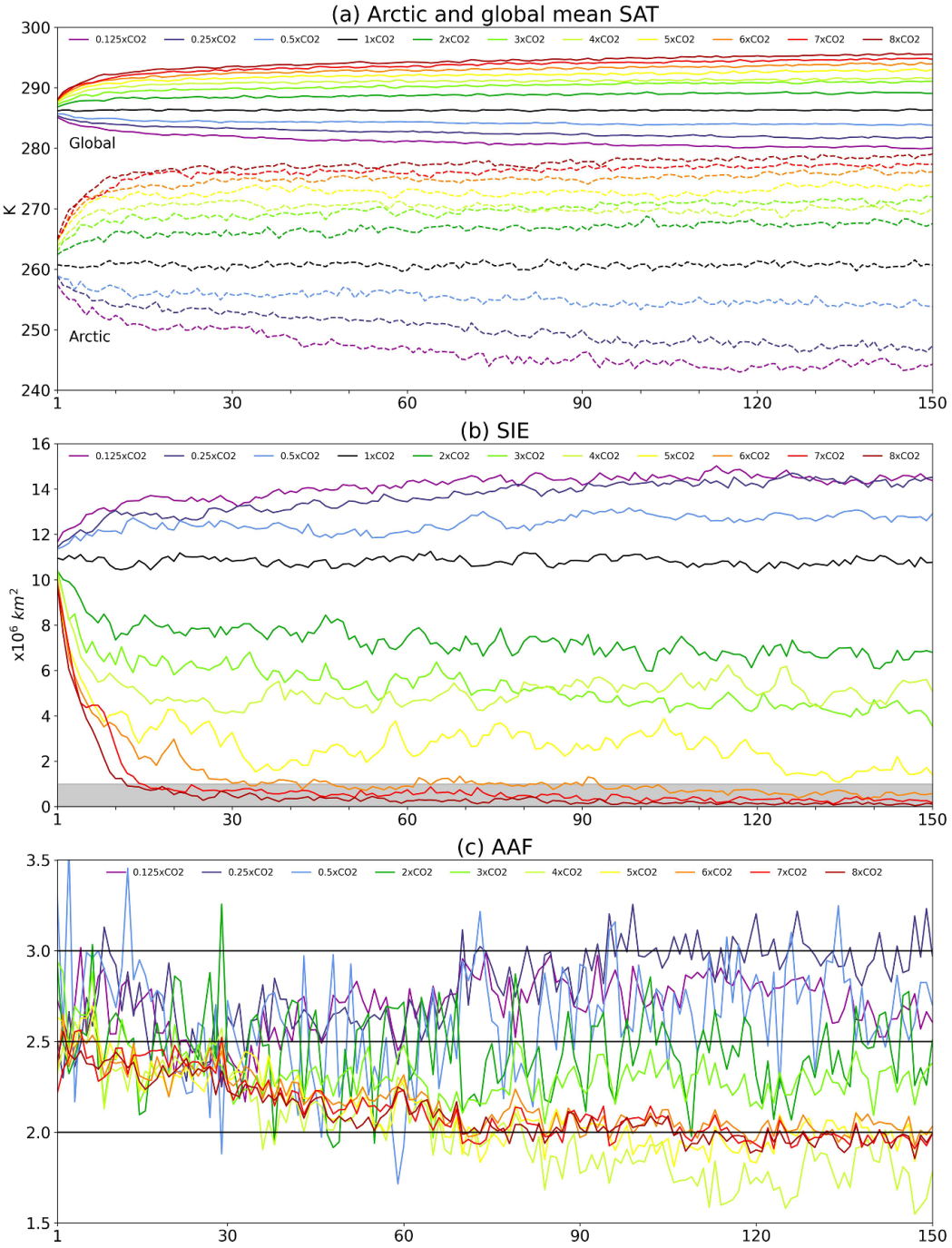

Figure 1. (a) Time series of Arctic and global annual-mean SATs for n×CO_2 experiments. (b) and (a): as in (a) but for Arctic annual-mean SIE, and annual AAF, respectively. The grey shading in (b) indicates the ice-free condition in which the SIE is less than 1000 000 km^2.

varying strength of CO_2 forcings. These variables behave consistently as a function of CO_2 forcing strength and are strongly connected to each other (black lines in figures 2(a)–(c). This manifests a known feedback process: the enhanced Arctic SAT due to increasing CO_2 level melts more sea ice and leads to more open ocean, allowing more ocean-to-atmosphere heat fluxes to warm the Arctic SAT further (e.g. Deser *et al* 2010, Screen and Simmonds 2010, Goosse *et al* 2018, Dai *et al* 2019, Deng *et al* 2020, Liang *et al* 2022a). If the Arctic SAT cools under decreasing CO_2 concentration, this feedback also works, evidenced by the 0.125×, 0.25×, and 0.5×CO_2 results.

It is noted that the kink in 4×CO_2 run is associated with the shutdown of Atlantic meridional overturning circulation (AMOC) (Mitevski *et al* 2021). Previous studies showed that many CMIP5 and

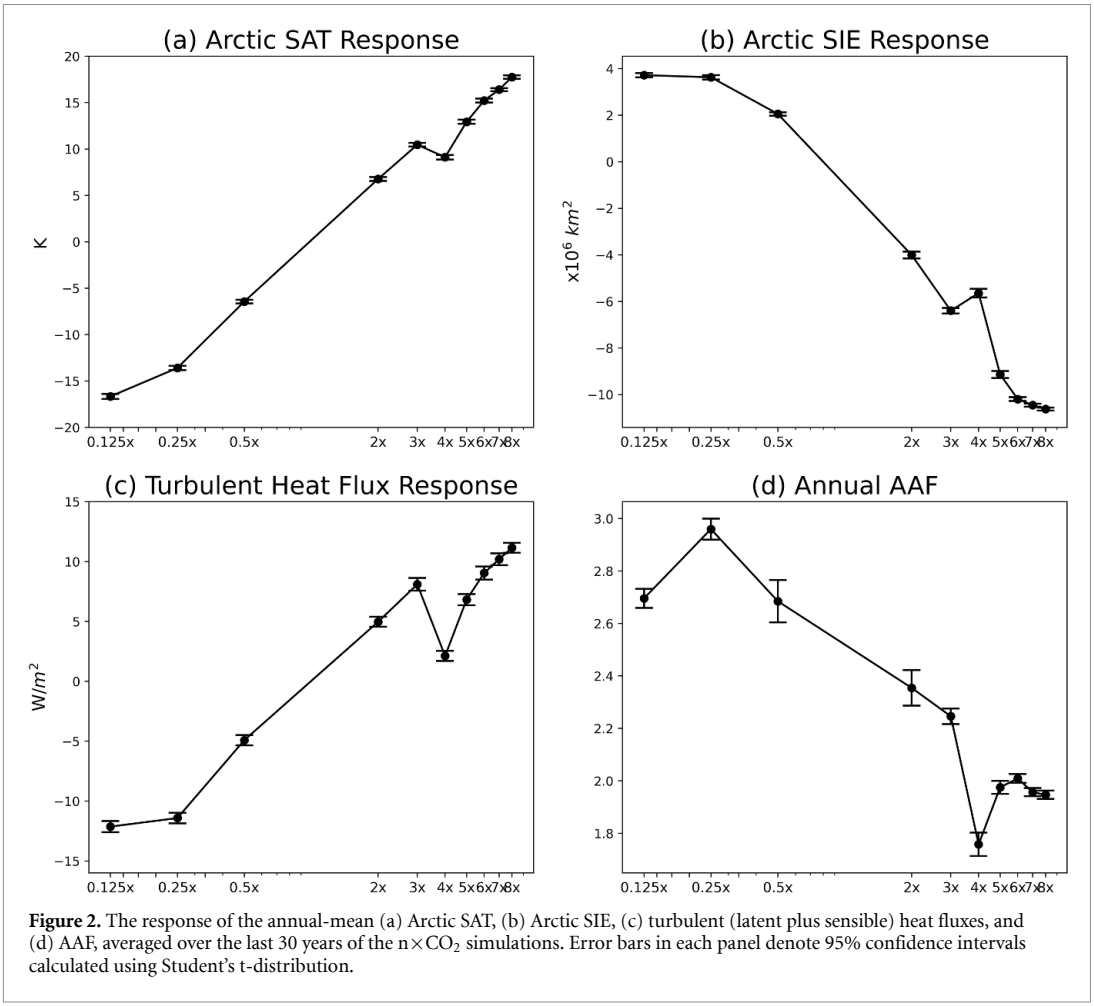

Figure 2. The response of the annual-mean (a) Arctic SAT, (b) Arctic SIE, (c) turbulent (latent plus sensible) heat fluxes, and (d) AAF, averaged over the last 30 years of the n×CO_2 simulations. Error bars in each panel denote 95% confidence intervals calculated using Student's t-distribution.

CMIP6 models exhibit significant weakening of the AMOC when CO_2 forcing increases (Rugenstein *et al* 2013, Winton *et al* 2013, Palter 2015, Trossman *et al* 2016, Caesar *et al* 2020). The reduction of Arctic sea ice could also influence the AMOC strength through increased freshwater fluxes, but this relationship is not unidirectional (Oudar *et al* 2017, Sévellec *et al* 2017, Sun *et al* 2018, Liu *et al* 2019). Focusing on CESM1 and GISS-E2.1-G under abrupt CO_2 forcing, Mitevski *et al* 2021 found that AMOC can collapse in 4×CO_2 and 3×CO_2 in the two models, respectively, and does not recover under stronger CO_2 forcings. Comparing with corresponding slab-ocean model experiments, they argued that the underlying mechanism is associated with the ocean dynamics.

Focusing on the AAF, the most important variable of this study, we find that the three cold AAFs are larger than any warm AAFs (figure 2(d)). The cold AAFs range between 2.7–3.0, whereas all warm AAFs are smaller than 2.4 in the measure of the 30 year mean. We also notice a reduction tendency in warm AAFs (except the 4×CO_2 case) as a function of CO_2 forcing strength, which is documented in previous studies and has been mainly attributed to the relatively smaller SIE decrease under a nearly ice-free condition and the accompanying weaker heat flux exchange between the ocean and atmosphere (Deser *et al* 2010, Screen and Simmonds 2010, Chung *et al* 2021, Liang *et al* 2022a). In contrast, unlike the warm AAFs (except the 4×CO_2 case) decreasing monotonically with increasing CO_2 concentrations, the largest cold AAF appears in the 0.25×CO_2 run rather than the 0.125×CO_2 run. Similarly, we attribute this to the relatively small SIE increase under a nearly ice-covered state, in which sea ice is hard to grow further when the CO_2 level declines further. Indeed, the SIE change between 0.125×CO_2 and 0.25×CO_2 runs is smaller than between 0.25×CO_2 and 0.5×CO_2 runs (figure 2(b)). Consequently, the turbulent heat fluxes and Arctic SAT changes are relatively small, giving rise to smaller AAF in the 0.125×CO_2 run than in the 0.25×CO_2 run. In addition, the AMOC collapse does have impact on the strength of AAF, as clearly shown in figure 2(d). And since the CO_2 radiative forcing still works on the climate system, despite the AMOC collapse, the associated feedbacks in Arctic region continue producing AA (see next paragraph).

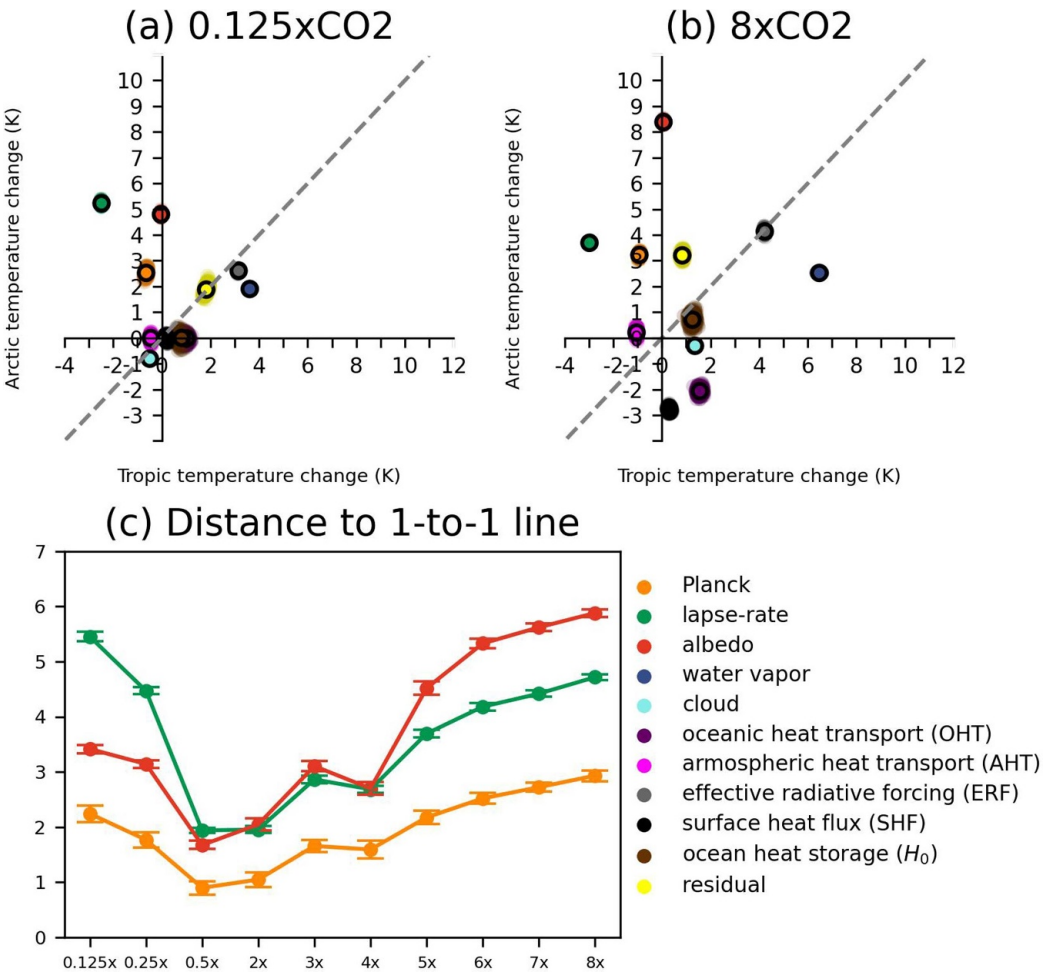

Figure 3. Contribution of feedbacks and meridional heat transports to the Arctic against tropical annual mean SATs under (a) abrupt $0.125\times CO_2$ and (b) $8\times CO_2$ forcing. In (a) and (b), the line with slope one (i.e. the one-to-one line) is plotted as a grey dashed line, and small dots are generated with 10 000 time random sampling for each feedback. (c) Distances to the one-to-one line for Planck, lapse-rate, and albedo feedbacks. In (c), error bars denote 95% confidence intervals calculated using Student's t-distribution.

The above results, having shed light on the mechanism associated with sea-ice retreat and ocean-to-atmosphere heat fluxes to produce cold and warm AAs, however, do not explicitly explain why cold AAF is larger than warm AAF. We, thus, perform a feedback analysis to seek the answer. For each feedback, ERF, and meridional heat transports, we plot its value averaged over the Arctic domain against that over the tropical domain following previous studies (e.g. Pithan and Mauritsen 2014, Hahn *et al* 2021, Beer and Eisenman 2022, Liang *et al* 2022b). Figures 3(a) and (b) show the results of $0.125\times CO_2$ and $8\times CO_2$ runs and compare their difference and similarity. The Planck, lapse-rate, and albedo feedbacks immediately stand out to be the major contributors to both cold and warm AAs because they are above the one-to-one line (grey dashed line), which informs the larger Arctic SAT change than the tropical (or global) one. In contrast, the water vapor feedback serves the role of de-AA. Other feedbacks and meridional heat transports do not play substantial roles in generating AA as they are close to the one-to-one line. We also perform the same analysis on other abrupt CO_2 runs and show the evolution of feedbacks with varying CO_2 levels in supplementary figures 1 and 2.

Let us now move back to the three feedbacks that are the main contributors to the cold and warm AAs. We find that their relative importance varies under decreasing and increasing CO_2 concentrations. Indeed, the lapse-rate feedback seems more influential than Planck and albedo feedbacks in $0.125\times CO_2$ run by looking at figure 3(a), while the Planck feedback seems equally important and the albedo feedback more important in $8\times CO_2$ run in figure 3(b). To quantify, we define the Euclidean distance to the one-to-one line as a measure of the 'importance' contributing to AA. Figure 3(c) presents how the distances of the three feedbacks evolve as a function of CO_2 forcing. It is clear that the lapse-rate feedback is stronger than the

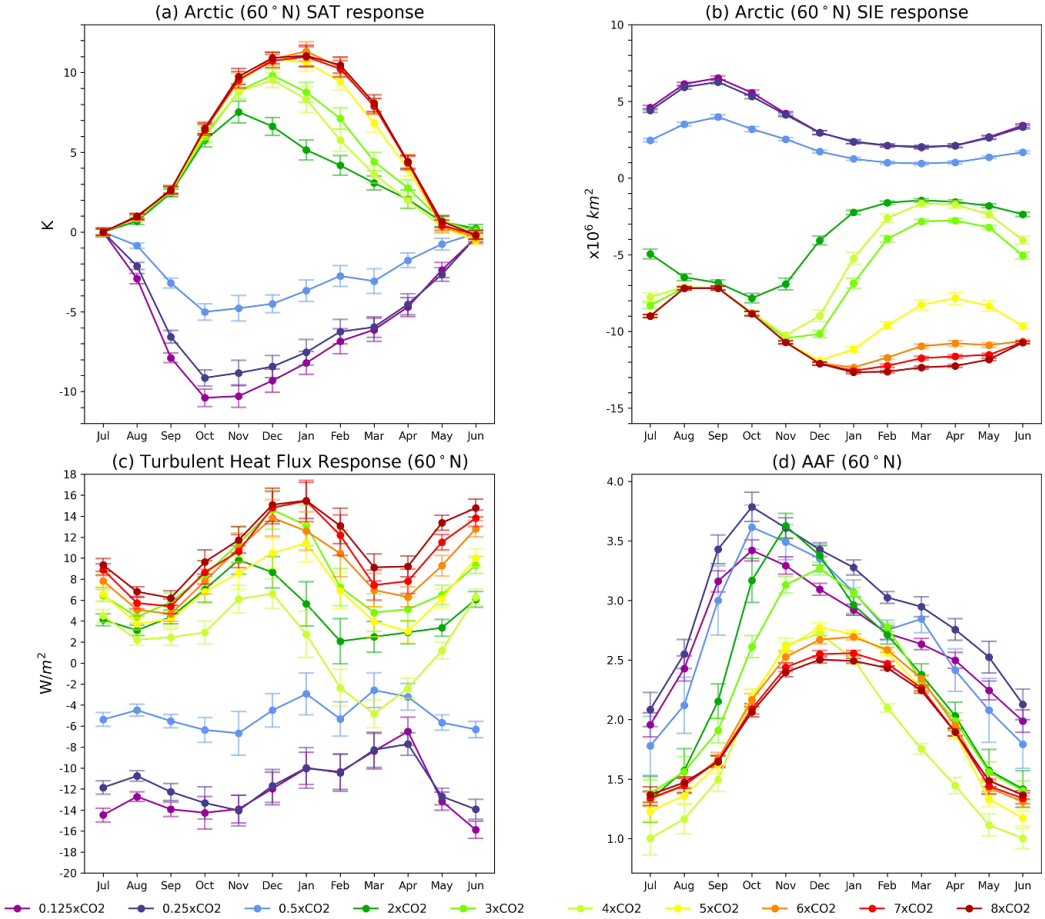

Figure 4. Seasonal migrations of (a) Arctic SAT response, (b) Arctic SIE response, (c) turbulent heat flux response, and (d) AAF. The error bars denote 95% confidence intervals calculated using Student's t-distribution.

albedo and Planck feedbacks in the cooling scenario, supported by the fact that it is statistically separable from the other feedbacks. The distance shrinks as the forcing strength is reduced. On the other hand, when the CO_2 concentration increases, the albedo feedback becomes more important than the other two feedbacks. These findings suggest that the stronger lapse-rate feedback under decreasing CO_2 forcing than increasing CO_2 forcing are the major contributors to producing a larger magnitude of AA.

To further investigate why the contributions of lapse-rate feedback vary, we look at the polar-cap and tropically-averaged vertical temperature profiles and their sensitivity with respect to global-mean SAT response. In particular, it is evident to see that the cooling scenarios give larger temperature difference between the lower and upper troposphere and stronger temperature inversion in the lower troposphere (supplementary figure 3(k)). This reveals the essence of stronger lapse-rate feedback produced by CO_2 reduction than that by CO_2 increase. For Planck feedback, we further analyze the spatial distribution of its parameters (supplementary figure 4). The spatial structure over the Arctic domain is somewhat different between warming and cooling simulations: in the warming scenarios, the large values occur between 85°N–90°N with magnitude weakened as increasing CO_2 concentration, whereas, in the cooling scenarios, between 70°N–80°N. Such spatial difference could be related to the sea-ice edge in the cooling and warming experiments. In contrast, less variations in spatial extent and magnitude are shown in the tropical domain (supplementary figure 4(a)). This suggests that the Planck feedback in the cooling scenarios has different spatial distribution in high latitudes than in the warming scenarios, although it plays similar role in producing AA.

Last but not least, we turn to contrasting the seasonality changes under decreasing and increasing CO_2 concentrations. Reported in Liang *et al* (2022a), the peak of Arctic SATs gradually migrates from November to December or January as CO_2 forcing increases (also see figure 4(a). However, not expected is that the peak of SATs under decreasing CO_2 levels does not shift its minimum value at all, indicating very weak or no apparent seasonality changes under the cooling scenario. The minimum of reduced SATs stays locked in

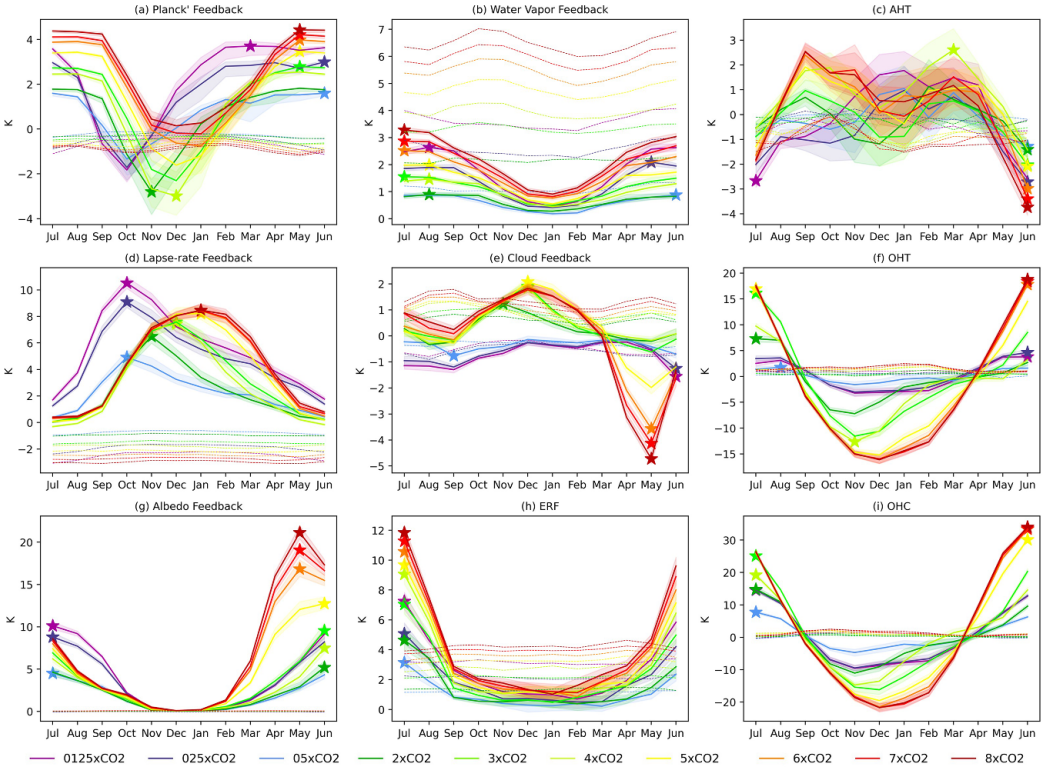

Figure 5. Seasonal migrations in temperature of (a) lapse-rate feedback, (b) water vapor feedback, (c) atmospheric heat transport (AHT), (d) Planck feedback, (e) cloud feedback, (f) oceanic heat transport (OHT), (g) albedo feedback, (h) effective radiative forcing (ERF) and (i) ocean heat storage (H_o) averaged over the Arctic domain. The color shadings denote 95% confidence intervals calculated using Student's t-distribution. The results averaged over the tropical domain are plotted as dashed lines. The largest values over the 12 months are marked as stars.

October, no matter whether the cooling forcing strength is enhanced. We also look into the responses of SIE and turbulent heat fluxes and find their seasonalities do not change much either (figures 4(b) and (c)). The maximum SIE responses occur in September, one month before minimum SAT responses, suggesting that SIE increase leads to weaker turbulent heat fluxes and cooler SAT. The reason why the SIE increase cannot move to an earlier month, for example, August, is likely related to the climatological SIE minimum in September, which locks the response phase in September. We also notice that the SIE responses are almost unchanged in $0.125\times CO_2$ and $0.25\times CO_2$ runs, consistent with their annual-mean SIE responses (figure 2(b)). This is probably caused by the increased SIE under the cooling scenario that almost fully covers the Arctic Ocean, limiting the degree of SIE change in all month. We also enlarge the domain to 55°N–90°N and obtain similar results (see supplementary figure 5) to make sure that the amount of sea-ice growth outside the Arctic domain we chose is not critical. As a consequence of the stagnation of Arctic SAT seasonality response to reduced CO_2 concentrations, the peaks of cold AAFs are locked in October (figure 4(d)).

To further investigate the associated processes other than the SIE-turbulent heat fluxes mechanism discussed above, we examine the seasonalities for all radiative feedbacks, ERF, AHT, and OHT. Only the lapse-rate feedback (figure 5(d)), identified as the second contributor to produce stronger cold AA (figure 3), shows consistent seasonality responses as those of the Arctic SAT and AAF: they do not shift their peaks in October under decreased CO_2 concentrations, while their peaks migrate gradually from November to January under increased CO_2 levels. Other feedbacks, ERF, and AHT, do not show consistent seasonality responses (figures 5(a), (b), (c), (e) and (h)), suggesting that they are not the main drivers of the AA seasonality changes. We also notice that OHT and H_o (figures 5(f) and (i)), show seasonal migration signature. The main reason underlying them is not clear, which we hope to examine in future studies. In addition, the spatial distribution of radiative feedback and temperature variability have been shown to influence AHT (Merlis *et al* 2022), which also deserve further examinations in the context of varying CO_2 levels.

However, it is difficult to interpret the causality that the lapse-rate feedback causes the seasonal changes of AA as there are no apparent lead-lag relationships between them and AAF. We, thus, argue that the lapse-rate feedback is not the main driver in modulating the AA seasonality change, but they play important roles in amplifying the seasonality responses (and are important for producing stronger cold AA). To test this argument, we look into both the lapse-rate feedback parameter and temperature inversion, defined as the difference between the air temperature at 850 hPa and 1000 hPa following Jenkins and Dai (2022). We find that they exhibit similar seasonal variations (supplementary figures 6(b) and (c)) to those of AA. This means that no apparent lead-lag relationship exists between them, suggesting the amplified Arctic warming and the associated vertical temperature profile is established almost immediately the lapse-rate feedback actually works. Therefore, the lapse-rate feedback may not be the essential driver for the AA seasonality shift. We also show that the tropics-averaged seasonality responses (dashed lines in figure 5) do not present strong seasonal dependence as those of Arctic ones. This means that the Arctic seasonality changes dominate the AAF seasonality changes.

4. Discussion

Our results not only demonstrate that the cold AA is stronger than the warm one, but also shed insight towards the asymmetric responses of Arctic climate change, as evidenced by the disproportional variations in its intensity and seasonality, to the increasing and decreasing CO_2 concentrations. The asymmetric responses in the Arctic resonate the asymmetry of global surface temperature to increasing and decreasing CO_2 levels presented in Mitevski *et al* (2022), which used the same abrupt CO_2 experiments under a broad range of CO_2 forcings. However, the underlying mechanism seems distinct as the asymmetric global temperature responses are mainly attributed to the non-logarithmic radiative forcing (Mitevski *et al* 2022), whereas this study finds that the asymmetric Arctic responses are related to the lapse-rate feedback. These reveal that the Arctic region is rather unique and needs to be studied separately from a global mean perspective. More efforts are needed to advance our understanding of the feedback processes and/or radiative forcing contributing to Arctic asymmetry, which could intrinsically build upon the non-linearity in Arctic climate response (e.g. Deng *et al* 2020, Sumata *et al* 2023).

Our findings of stronger cold AA may have implications for the effects of various CO_2 removal or net-zero emissions scenarios (Oh *et al* 2022), instigated by the 2015 Paris Agreement with a pursuit to limit the global temperature increase to 1.5 °C above PI levels, on Arctic climate change. To achieve this objective, net negative CO_2 emissions are demanded (Hoegh-Guldberg *et al* 2018), so a stronger cold AA signature could emerge. Our results may also pave a road for investigating the effects of anthropogenic aerosol emissions on Arctic climate change. Although the aerosol radiative forcing is somewhat different from CO_2 forcing in terms of geographical distribution and temporal evolution, both previous and recent studies revealed that the cooling induced by the aerosol loading likely gives rise to cold AA (Feichter *et al* 2004, Ming and Ramaswamy 2009, Deng *et al* 2020, Jiang *et al* 2020, England *et al* 2021). Whether or not the cold AA produced by anthropogenic aerosol emissions is stronger than that by CO_2 emission or removal remains an open question and yet to be examined. Our findings, thus, have significant implications for how the carbon removal or the effects of anthropogenic aerosol emissions could impact Arctic climate, ecosystems, and socio-economic activities.

For the feedback analysis, we use the radiative kernel technique (Soden *et al* 2008) to quantify the roles of radiative feedbacks in contributing to cold and warm AAs. However, the radiative kernel could be limited to state-dependent issue. A study using MPI-ESM-LR radiative kernel showed that the strength of albedo feedback is reduced by 50% comparing the $4\times CO_2$ run with the control PI run (Block and Mauritsen 2013), indicating that the albedo feedback is state-dependent. Indeed, we find that the albedo feedback becomes less important in $2\times CO_2$ and $0.5\times CO_2$ cases. Jonko *et al* (2013) further decomposed the contribution of each feedback into the a radiative flux change and a climatic response to temperature change using kernel technique. They showed that the variations in Planck and water vapor feedbacks are largely due to changes in the radiative flux associated with varying climate state. We also notice that the residuals, not ignorable, vary in the Arctic averages when the CO_2 concentration chagnes (see supplementary figure 1), reflecting the variations of radiative kernel technique in polar averages also shown in Jonko *et al* (2013). Lastly, the different selection of baseline climate state from the PI control run could affect the relative importance of each feedback. As such, the legitimacy of the kernel applied to both warming and cooling states needs to be investigated further. Moreover, the linear decomposition of the radiative kernel technique may not properly account for the non-linear interactions between feedbacks (Goosse *et al* 2018, Henry *et al* 2021, Beer and Eisenman 2022) and the coupling between feedbacks and meridional heat transports (e.g. Langen *et al* 2012, Merlis 2014, Feldl *et al* 2020, Russotto and Biasutti 2020). Other techniques, in particular, the coupled

atmosphere–surface climate feedback–response analysis method (Cai and Lu 2009, Lu and Cai 2009a), the feedback-locking method (Hall 2004, Graversen and Wang 2009, Middlemas *et al* 2020, Beer and Eisenman 2022), and the moist energy balance model (Hwang and Frierson 2010, Hwang *et al* 2011, Rose *et al* 2014, Roe *et al* 2015, Bonan *et al* 2018, Russotto and Biasutti 2020), can be considered in future works to revisit the findings of this study.

5. Conclusion

This study, for the first time, has contrasted the cold AA to the warm AA using a series of abrupt CO_2 experiments, conducted with a state-of-the-art fully coupled climate model. We not only illustrated the phenomenological characteristics of cold AA, but also examined the underlying mechanisms. The main finding, perhaps surprisingly, is that decreasing, rather than increasing, CO_2 concentrations produce stronger AA. We showed that the sea-ice loss-turbulent heat fluxes-SAT feedback play an essential role in producing both cold and warm AAs, but cannot explicitly explain why the cold AA is stronger. The feedback analysis suggests that the stronger lapse-rate feedback in the cooling scenario compared to the warming scenario are the major contributors to generating stronger AA.

We have also examined the seasonality of the responses to decreasing and increasing CO_2. Unlike the peaks of warm AA, which shift gradually from November to December or January as CO_2 increases, those of cold AA do not shift but are locked in the month of October. We attribute this apparent phase-locking to a nearly ice-covered Arctic Ocean under the cooling scenario that limits the degree of SIE seasonal changes, as well as the climatological SIE minimum in September. And finally, we have found that the lapse-rate feedback amplifies the AA seasonality response, but may not be the essential driver.

Data availability statement

The data of abrupt CO_2 experiments can be obtained at https://doi.org/10.5281/zenodo.5725084. The plotting Python scripts can be downloaded from https://doi.org/10.5281/zenodo.7763116, or upon request to the corresponding author.

Acknowledgments

S-N Zhou and Y-C Liang are supported by grants from the Ministry of Science and Technology (110-2111-M-002-019-MY2 and 111-2628-M-002-011) to National Taiwan University. I Mitevski is supported by NASA FINESST Grant 80NSSC20K1657. L M Polvani acknowledges support from a grant from the US National Science Foundation to Columbia University. We would like to acknowledge high-performance computing support from Cheyenne (doi:https://doi.org/10.5065/D6RX99HX) provided by NCAR's Computational and Information Systems Laboratory, sponsored by the National Science Foundation. We thank the editor and two anonymous reviewers for their constructive comments and suggestions to improve the quality of this manuscript.

Conflict of interest

The authors have no conflicts of interest to report.

ORCID iDs

Yu-Chiao Liang https://orcid.org/0000-0002-9347-2466
Lorenzo M Polvani https://orcid.org/0000-0003-4775-8110

References

Alvarez J, Yumashev D and Whiteman G 2020 A framework for assessing the economic impacts of Arctic change *Ambio* **49** 407–18
Barnes E A 2013 Revisiting the evidence linking Arctic amplification to extreme weather in midlatitudes *Geophys. Res. Lett.* **40** 4734–9
Barnes E A and Screen J A 2015 The impact of Arctic warming on the midlatitude jet-stream: can it? Has it? Will it? *Wiley Interdiscip. Rev. Clim. Change* **6** 277–86
Beer E and Eisenman I 2022 Revisiting the role of the water vapor and lapse rate feedbacks in the Arctic amplification of climate change *J. Clim.* **35** 2975–88
Blackport R and Screen J A 2020a Insignificant effect of Arctic amplification on the amplitude of midlatitude atmospheric waves *Sci. Adv.* **6** eaay2880
Blackport R and Screen J A 2020b Weakened evidence for mid-latitude impacts of Arctic warming *Nat. Clim. Change* **10** 1065–6
Blackport R, Screen J A, van der Wiel K and Bintanja R 2019 Minimal influence of reduced Arctic sea ice on coincident cold winters in mid-latitudes *Nat. Clim. Change* **9** 697–704

Block K and Mauritsen T 2013 Forcing and feedback in the MPI-ESM-LR coupled model under abruptly quadrupled CO_2 *J. Adv. Model. Earth Syst.* **5** 676–91
Boeke R C and Taylor P C 2018 Seasonal energy exchange in sea ice retreat regions contributes to differences in projected Arctic warming *Nat. Commun.* **9** 5017
Bonan D, Armour K, Roe G, Siler N and Feldl N 2018 Sources of uncertainty in the meridional pattern of climate change *Geophys. Res. Lett.* **45** 9131–40
Burgass M J, Milner-Gulland E, Stewart Lowndes J S, O'Hara C, Afflerbach J C and Halpern B S 2019 A pan-Arctic assessment of the status of marine social-ecological systems *Reg. Environ. Change* **19** 293–308
Caesar L, Rahmstorf S and Feulner G 2020 On the relationship between atlantic meridional overturning circulation slowdown and global surface warming *Environ. Res. Lett.* **15** 024003
Cai M and Lu J 2009 A new framework for isolating individual feedback processes in coupled general circulation climate models. Part II: method demonstrations and comparisons *Clim. Dyn.* **32** 887–900
Cai Z, You Q, Wu F, Chen H W, Chen D and Cohen J 2021 Arctic warming revealed by multiple CMIP6 models: evaluation of historical simulations and quantification of future projection uncertainties *J. Clim.* **34** 4871–92
Chung E-S, Ha K-J, Timmermann A, Stuecker M F, Bodai T and Lee S-K 2021 Cold-season Arctic amplification driven by Arctic ocean-mediated seasonal energy transfer *Earth's Future* **9** e2020EF001898
Chylek P, Folland C, Klett J D, Wang M, Hengartner N, Lesins G and Dubey M K 2022 Annual mean Arctic amplification 1970–2020: observed and simulated by CMIP6 climate models *Geophys. Res. Lett.* **49** e2022GL099371
Cohen J *et al* 2014 Recent Arctic amplification and extreme mid-latitude weather *Nat. Geosci.* **7** 627–37
Cohen J *et al* 2020 Divergent consensuses on Arctic amplification influence on midlatitude severe winter weather *Nat. Clim. Change* **10** 20–29
Cohen J, Pfeiffer K and Francis J A 2018 Warm Arctic episodes linked with increased frequency of extreme winter weather in the United States *Nat. Commun.* **9** 869
Collins M *et al* 2013 Long-term climate change: projections, commitments and irreversibility *Climate change 2013: The Physical Science Basis*, ed T F Stocker *et al* pp 1029–136
Coumou D, Di Capua G, Vavrus S, Wang L and Wang S 2018 The influence of arctic amplification on mid-latitude summer circulation *Nat. Commun.* **9** 2959
Dai A, Luo D, Song M and Liu J 2019 Arctic amplification is caused by sea-ice loss under increasing CO_2 *Nat. Commun.* **10** 121
Davy R and Outten S 2020 The Arctic surface climate in CMIP6: status and developments since CMIP5 *J. Clim.* **33** 8047–68
Deng J, Dai A and Xu H 2020 Nonlinear climate responses to increasing CO_2 and anthropogenic aerosols simulated by CESM1 *J. Clim.* **33** 281–301
Deser C, Tomas R, Alexander M and Lawrence D 2010 The seasonal atmospheric response to projected Arctic sea ice loss in the late twenty-first century *J. Clim.* **23** 333–51
England M R, Eisenman I, Lutsko N J and Wagner T J W 2021 The recent emergence of Arctic amplification *Geophys. Res. Lett.* **48** e2021GL094086
Eyring V, Bony S, Meehl G A, Senior C A, Stevens B, Stouffer R J and Taylor K E 2016 Overview of the coupled model intercomparison project phase 6 (CMIP6) experimental design and organization *Geosci. Model Dev.* **9** 1937–58
Feichter J, Roeckner E, Lohmann U and Liepert B 2004 Nonlinear aspects of the climate response to greenhouse gas and aerosol forcing *J. Clim.* **17** 2384–98
Feldl N, Po-Chedley S, Singh H K A, Hay S and Kushner P J 2020 Sea ice and atmospheric circulation shape the high-latitude lapse rate feedback *npj Clim. Atmos. Sci.* **3** 41
Francis J A and Vavrus S J 2012 Evidence linking Arctic amplification to extreme weather in mid-latitudes *Geophys. Res. Lett.* **39** 6
Gillett N P, Stone D A, Stott P A, Nozawa T, Karpechko A Y, Hegerl G C, Wehner M F and Jones P D 2008 Attribution of polar warming to human influence *Nat. Geosci.* **1** 750–4
Goosse H *et al* 2018 Quantifying climate feedbacks in polar regions *Nat. Commun.* **9** 1919
Graversen R G and Wang M 2009 Polar amplification in a coupled climate model with locked albedo *Clim. Dyn.* **33** 629–43
Hahn L C, Armour K C, Battisti D S, Eisenman I and Bitz C M 2022 Seasonality in Arctic warming driven by sea ice effective heat capacity *J. Clim.* **35** 1629–42
Hahn L C, Armour K C, Zelinka M D, Bitz C M and Donohoe A 2021 Contributions to polar amplification in CMIP5 and CMIP6 models *Front. Earth Sci.* **9** 710036
Hall A 2004 The role of surface albedo feedback in climate *J. Clim.* **17** 1550–68
Henry M, Merlis T M, Lutsko N J and Rose B E J 2021 Decomposing the drivers of polar amplification with a single-column model *J. Clim.* **34** 2355–65
Hoegh-Guldberg O *et al* 2018 Impacts of 1.5 °C global warming on natural and human systems *Global Warming of 1.5 °C* (IPCC Secretariat)
Hoffert M I and Covey C 1992 Deriving global climate sensitivity from palaeoclimate reconstructions *Nature* **360** 573–6
Holland M M and Landrum L 2021 The emergence and transient nature of Arctic amplification in coupled climate models *Front. Earth Sci.* **9** 719024
Hu X, Liu Y, Kong Y and Yang Q 2022 A quantitative analysis of the source of inter-model spread in Arctic surface warming response to increased CO_2 concentration *Geophys. Res. Lett.* **49** e2022GL100034
Hwang Y-T and Frierson D M W 2010 Increasing atmospheric poleward energy transport with global warming *Geophys. Res. Lett.* **37** 24
Hwang Y-T, Frierson D M W and Kay J E 2011 Coupling between Arctic feedbacks and changes in poleward energy transport *Geophys. Res. Lett.* **38** 17
Jenkins M T and Dai A 2022 Arctic climate feedbacks in ERA5 reanalysis: seasonal and spatial variations and the impact of sea-ice loss *Geophys. Res. Lett.* **49** e2022GL099263
Jenkins M and Dai A 2021 The impact of sea-ice loss on Arctic climate feedbacks and their role for Arctic amplification *Geophys. Res. Lett.* **48** e2021GL094599
Jiang Y, Yang X-Q, Liu X, Qian Y, Zhang K, Wang M, Li F, Wang Y and Lu Z 2020 Impacts of wildfire aerosols on global energy budget and climate: the role of climate feedbacks *J. Clim.* **33** 3351–66
Jones G S, Stott P A and Christidis N 2013 Attribution of observed historical near–surface temperature variations to anthropogenic and natural causes using CMIP5 simulations *J. Geophys. Res.* **118** 4001–24
Jonko A K, Shell K M, Sanderson B M and Danabasoglu G 2013 Climate feedbacks in CCSM3 under changing CO_2 forcing. Part II: variation of climate feedbacks and sensitivity with forcing *J. Clim.* **26** 2784–95

Kay J E et al 2015 The community earth system model (CESM) large ensemble project: a community resource for studying climate change in the presence of internal climate variability *Bull. Am. Meteorol. Soc.* **96** 1333–49
Langen P L, Graversen R G and Mauritsen T 2012 Separation of contributions from radiative feedbacks to polar amplification on an aquaplanet *J. Clim.* **25** 3010–24
Lenssen N J L, Schmidt G A, Hansen J E, Menne M J, Persin A, Ruedy R and Zyss D 2019 Improvements in the GISTEMP uncertainty model *J. Geophys. Res.* **124** 6307–26
Liang Y-C, Polvani L M and Mitevski I 2022a Arctic amplification and its seasonal migration, over a wide range of abrupt CO_2 forcing *npj Clim. Atmos. Sci.* **5** 14
Liang Y-C, Polvani L M, Previdi M, Smith K L, England M R and Chiodo G 2022b Stronger Arctic amplification from ozone-depleting substances than from carbon dioxide *Environ. Res. Lett.* **17** 024010
Liu W, Fedorov A and Sévellec F 2019 The mechanisms of the atlantic meridional overturning circulation slowdown induced by Arctic sea ice decline *J. Clim.* **32** 977–96
Lu J and Cai M 2009a A new framework for isolating individual feedback processes in coupled general circulation climate models. Part I: formulation *Clim. Dyn.* **32** 873–85
Lu J and Cai M 2009b Seasonality of polar surface warming amplification in climate simulations *Geophys. Res. Lett.* **36** 16
Manabe S and Stouffer R J 1980 Sensitivity of a global climate model to an increase of CO_2 concentration in the atmosphere *J. Geophys. Res. Oceans* **85** 5529–54
Manabe S and Wetherald R T 1975 The effects of doubling the CO_2 concentration on the climate of a general circulation model *J. Atmos. Sci.* **32** 3–15
Meredith M *et al* 2019 Polar regions. Chapter 3, IPCC special report on the ocean and cryosphere in a changing climate (available at: www.ipcc.ch/srocc/chapter/chapter-3-2/)
Merlis T M 2014 Interacting components of the top-of-atmosphere energy balance affect changes in regional surface temperature *Geophys. Res. Lett.* **41** 7291–7
Merlis T M, Feldl N and Caballero R 2022 Changes in poleward atmospheric energy transport over a wide range of climates: energetic and diffusive perspectives and a priori theories *J. Clim.* **35** 6533–48
Middlemas E, Kay J, Medeiros B and Maroon E 2020 Quantifying the influence of cloud radiative feedbacks on Arctic surface warming using cloud locking in an earth system model *Geophys. Res. Lett.* **47** e2020GL089207
Miller G H, Alley R B, Brigham-Grette J, Fitzpatrick J J, Polyak L, Serreze M C and White J W C 2010 Arctic amplification: can the past constrain the future? *Quat. Sci. Rev.* **29** 1779–90
Ming Y and Ramaswamy V 2009 Nonlinear climate and hydrological responses to aerosol effects *J. Clim.* **22** 1329–39
Mitevski I, Orbe C, Chemke R, Nazarenko L and Polvani L M 2021 Non-monotonic response of the climate system to abrupt CO_2 forcing *Geophys. Res. Lett.* **48** e2020GL090861
Mitevski I, Polvani L M and Orbe C 2022 Asymmetric warming/cooling response to CO_2 increase/decrease mainly due to non-logarithmic forcing, not feedbacks *Geophys. Res. Lett.* **49** e2021GL097133
Mori M, Watanabe M, Shiogama H, Inoue J and Kimoto M 2014 Robust Arctic sea-ice influence on the frequent Eurasian cold winters in past decades *Nat. Geosci.* **7** 869–73
Oh J-H, An S-I, Shin J and Kug J-S 2022 Centennial memory of the Arctic ocean for future Arctic climate recovery in response to a carbon dioxide removal *Earth's Future* **10** e2022EF002804
Oudar T, Sanchez-Gomez E, Chauvin F, Cattiaux J, Terray L and Cassou C 2017 Respective roles of direct GHG radiative forcing and induced Arctic sea ice loss on the northern hemisphere atmospheric circulation *Clim. Dyn.* **49** 3693–713
Overland J E, Dethloff K, Francis J A, Hall R J, Hanna E, Kim S-J, Screen J A, Shepherd T G and Vihma T 2016 Nonlinear response of mid-latitude weather to the changing Arctic *Nat. Clim. Change* **6** 992–9
Overland J, Francis J A, Hall R, Hanna E, Kim S-J and Vihma T 2015 The melting Arctic and midlatitude weather patterns: are they connected? *J. Clim.* **28** 7917–32
Palter J B 2015 The role of the gulf stream in European climate *Annu. Rev. Mar. Sci.* **7** 113–37
Park H-S, Kim S-J, Stewart A L, Son S-W and Seo K-H 2019 Mid-holocene northern hemisphere warming driven by Arctic amplification *Sci. Adv.* **5** eaax8203
Pedregosa F *et al* 2011 Scikit-learn: machine learning in python *J. Mach. Learn. Res.* **12** 2825–30 (available at: www.jmlr.org/papers/volume12/pedregosa11a/pedregosa11a.pdf?ref=https:/)
Pendergrass A G, Conley A and Vitt F M 2018 Surface and top-of-atmosphere radiative feedback kernels for CESM-CAM5 *Earth Syst. Sci. Data* **10** 317–24
Pithan F and Mauritsen T 2014 Arctic amplification dominated by temperature feedbacks in contemporary climate models *Nat. Geosci.* **7** 181–4
Polvani L M, Previdi M, England M R, Chiodo G and Smith K L 2020 Substantial twentieth-century Arctic warming caused by ozone-depleting substances *Nat. Clim. Change* **10** 130–3
Previdi M, Janoski T P, Chiodo G, Smith K L and Polvani L M 2020 Arctic amplification: a rapid response to radiative forcing *Geophys. Res. Lett.* **47** e2020GL089933
Rantanen M, Karpechko A Y, Lipponen A, Nordling K, Hyvärinen O, Ruosteenoja K, Vihma T and Laaksonen A 2022 The Arctic has warmed nearly four times faster than the globe since 1979 *Commun. Earth Environ.* **3** 168
Roe G H, Feldl N, Armour K C, Hwang Y-T and Frierson D M W 2015 The remote impacts of climate feedbacks on regional climate predictability *Nat. Geosci.* **8** 135–9
Rose B E J, Armour K C, Battisti D S, Feldl N and Koll D D B 2014 The dependence of transient climate sensitivity and radiative feedbacks on the spatial pattern of ocean heat uptake *Geophys. Res. Lett.* **41** 1071–8
Rugenstein M A A, Winton M, Stouffer R J, Griffies S M and Hallberg R 2013 Northern high-latitude heat budget decomposition and transient warming *J. Clim.* **26** 609–21
Russotto R D and Biasutti M 2020 Polar amplification as an inherent response of a circulating atmosphere: results from the tracmip aquaplanets *Geophys. Res. Lett.* **47** e2019GL086771
Screen J A and Simmonds I 2010 Increasing fall-winter energy loss from the Arctic ocean and its role in Arctic temperature amplification *Geophys. Res. Lett.* **37** 16
Serreze M C and Francis J A 2006 The Arctic amplification debate *Clim. Change* **76** 241–64
Serreze M, Barrett A, Stroeve J, Kindig D and Holland M 2009 The emergence of surface-based Arctic amplification *Cryosphere* **3** 11–19
Sévellec F, Fedorov A V and Liu W 2017 Arctic sea-ice decline weakens the atlantic meridional overturning circulation *Nat. Clim. Change* **7** 604–10

Sloan L C and Rea D 1996 Atmospheric carbon dioxide and early eocene climate: a general circulation modeling sensitivity study *Palaeogeogr. Palaeoclimatol. Palaeoecol.* **119** 275–92
Smith D M *et al* 2022 Robust but weak winter atmospheric circulation response to future Arctic sea ice loss *Nat. Commun.* **13** 727
Soden B J, Held I M, Colman R, Shell K M, Kiehl J T and Shields C A 2008 Quantifying climate feedbacks using radiative kernels *J. Clim.* **21** 3504–20
Sumata H, de Steur L, Divine D V, Granskog M A and Gerland S 2023 Regime shift in Arctic ocean sea ice thickness *Nature* **615** 443–9
Sun L, Alexander M and Deser C 2018 Evolution of the global coupled climate response to Arctic sea ice loss during 1990–2090 and its contribution to climate change *J. Clim.* **31** 7823–43
Taylor P C *et al* 2022 Process drivers, inter-model spread and the path forward: a review of amplified Arctic warming *Frontiers Earth Sci.* **9** 758361
Trossman D, Palter J, Merlis T, Huang Y and Xia Y 2016 Large-scale ocean circulation-cloud interactions reduce the pace of transient climate change *Geophys. Res. Lett.* **43** 3935–43
Whiteman G and Yumashev D 2018 Poles apart: the arctic & management studies *J. Manage. Stud.* **55** 873–9
Winton M, Griffies S M, Samuels B L, Sarmiento J L and Frölicher T L 2013 Connecting changing ocean circulation with changing climate *J. Clim.* **26** 2268–78
Wu Y-T, Liang Y-C, Kuo Y-N, Lehner F, Previdi M, Polvani L M, Lo M-H and Lan C-W 2023 Exploiting smiles and the CMIP5 archive to understand Arctic climate change seasonality and uncertainty *Geophys. Res. Lett.* **50** e2022GL100745
Zappa G, Ceppi P and Shepherd T G 2021 Eurasian cooling in response to Arctic sea-ice loss is not proved by maximum covariance analysis *Nat. Clim. Change* **11** 106–8